WORLD METEOROLOGICAL ORGANIZATION
WEATHER CLIMATE WATER
CIMO TECHNICAL CONFERENCE ON METEOROLOGICAL AND ENVIRONMENTAL INSTRUMENTS AND METHODS OF OBSERVATION (CIMO TECO-2018)

Remote Measurements of Volcanic Plume Electrification Using a Sparse Network Technique

Jeff Lapierre[1], Alexa R. Van Eaton[2], Michael Stock[1], Matthew M. Haney[3], and John J. Lyons[3]
[1]Earth Networks
[2]U.S. Geological Survey, Cascades Volcano Observatory, Vancouver WA 98683 USA
[3]U.S. Geological Survey, Alaska Volcano Observatory, Anchorage, AK 99508 USA

***Abstract*— Ash from explosive volcanic eruptions can affect our environment by disrupting airline flights and marine traffic, reducing air quality, and impacting downwind communities. Understanding the processes occurring during eruptions can help mitigate these hazards by giving early warning of the eruption onset and improving the forecasts of ash dispersal. An emerging tool in this approach is volcanic lightning detection. Recent field campaigns have focused on how to link electrification to eruption dynamics such as mass flux, water content, and microphysical processes (e.g., volcanic hail formation). However, many volcanoes are remote and lack local monitoring equipment, making fine-scale electrical measurements particularly challenging. Here, we present a new technique to detect volcanic electrification that requires only two wideband radiofrequency sensors located within approximately 1,000 km of the volcano. The technique calculates the expected time delay of the signal between the two sensors, and from the volcano under observation. With this time delay, a cross-correlation can be applied to determine signals of possible volcanic origin. The sensors used in this study are from the Earth Networks Total Lightning Network (ENTLN), which are wideband electric field sensors in the range of 5–500 kHz. To demonstrate the technique, we examine the eruption of Bogoslof volcano in Alaska and specifically the explosive event on June 10th, 2017. We also investigate the likelihood and origin of false positives. Initial results indicate that this technique can detect many electrical discharges that were filtered out by the ENTLN operational algorithm or were not detected by other global lightning detection networks. An important implication is that this technique could reduce the latency of eruption alerts indicating that significant ash emissions have begun, and increase the number of detected discharges available to characterize the eruption dynamics in near-real time. We suggest this technique could be used operationally as part of an eruption monitoring system, which would be especially useful for volcanoes that are not currently instrumented.**

Keywords - lightning; volcano; electrification; volcanic ash

I. INTRODUCTION

Volcanic plumes from powerful eruptions commonly become electrified and produce lightning due to charging of ash particles at different stages of plume development [Thomas et al. 2010; Behnke et al. 2013]. Lightning produces radio emissions that are relatively easy to detect over long distances. For this reason, volcanic lightning is increasingly being used as a tool for characterizing explosive eruptions [Behnke and McNutt 2014; Fee et al., 2017; Haney et al., 2018]. However, many volcanoes are located in remote areas with sparse networks of lightning sensors, which makes it difficult and costly to detect their electrical activity.

The goal of this study is to develop a new form of lightning detection for regions with sparse network coverage. The data used for this study comes from the Earth Networks Total Lightning Network (ENTLN), which archives the raw waveform data needed for this technique. Here, we describe the approach, validate the results with two other long-range lightning detection networks, and consider the broader implications for volcano monitoring.

II. DATA

A. Earth Networks Total Lightning Network

The ENTLN continuously measures lightning stroke occurrence time, location, type (IC and CG), polarity, and peak current. The ENTLN network consists of over 1,600 ground-based wideband sensors around the world to detect both the IC and CG lightning, having a detection efficiency for IC strokes of up to 95% [Liu et al. 2010] and CG strokes of up to 97% [Zhu et. al. 2017]. These peak detection efficiencies are located over the central and eastern U.S., where the sensors are densest, and varies depending on network coverage. The region of this study, the Aleutian Islands in Alaska, is quite remote. As such, ENTLN only has a few sensors in the surrounding area and the detection efficiency will be much lower than the referenced values above.

ENTLN archives the electric field waveforms from each sensor. These waveforms allow for the unique opportunity to apply the technique developed in this study. We use data from two sensors, named UNLSK and USGS01, that are 98 and 622 km away from Bogoslof volcano, respectively. The map showing the location of the volcano and the two sensors is shown in Figure 1.

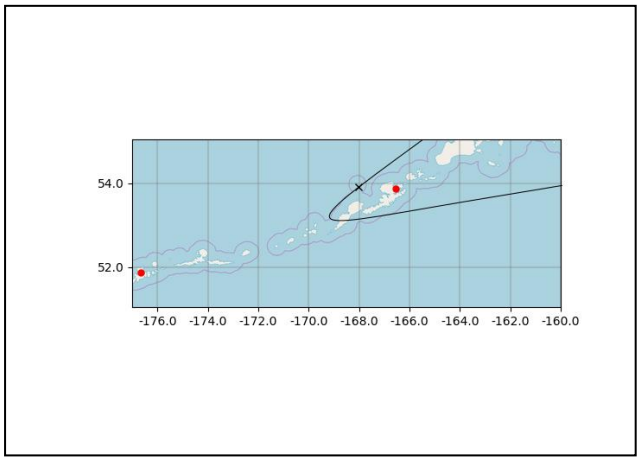

Figure 1. Map of Bogoslof volcano (X) and both ENTLN sensors (red dots). The black line is an approximaton of the hyperbolic equation describing the time-of-arrival solutions using two stations.

B. Lightning Location Datasets

As validation for this new method, we use lightning location data from two systems, which will be referenced as LLS1 and LLS2 in this paper. Both systems measure very low frequency radio signals and can detect lightning over long range (~2000-3000 km). This allows for detections in remote regions such as Bogoslof volcano.

III. METHODOLOGY

The technique used in this study relies on the cross-correlation of electric field waveform data from two ENTLN sensors. Cross-correlation measures how similar two waveforms are when a specific time offset is applied. In this case, the time offset between the two sensors is known since the location of the source (Bogosolf volcano), as well as the wave velocity (speed of light) is known. In comparison, most lightning location systems, including the two used in this study, use time-of-arrival and/or magnetic direction-finding techniques to locate lightning, which requires are least 3 sensors to provide a location. In the case of cross-correlation, only two sensors are required, though any signal with the same delay time will also trigger a detection. The solution for time-of-arrival using two sensors is a hyperbola [Drake et. al. 2004] and crosses in between the two sensors (see Figure 1). Any source that is also on that line will have the same time delay as that from Bogoslof volcano and result in a false detection.

To test for the presence of a signal at a given location, a cross-correlation is used and is given by,

$$Xc = \Sigma \left(x[t] * y[t-\tau]\right) / \left(\text{sqrt}(\Sigma\, x[t]^2) * \text{sqrt}(\Sigma\, y[t]^2)\right)$$

Where x and y are the normalized waveform data from the closest and farthest sensor, respectively, τ is the expected delay between the stations given the expected location of Bogoslof, t are the times of the samples of closest sensor. The denominator acts to normalize the cross-correlation between +/- 1. In general, t-τ will not correspond to an even sample time of y, so the amplitude of y at this time is found using linear interpolation. Further, because the waveform data use non-uniform sampling as part of the data compression routine, Xc(x,y) != -Xc(y,x). However, both terms will have local maxima if a source exists at the test location. The cross-correlation is calculated for every data point of the waveform from the closest station and using a 5 ms time window.

Once the cross-correlations are calculated, these data are used to characterize lightning pulses granted certain requirements are met. First, the cross-correlation must be above one standard deviation. Next, a "pulse" must be at least 10 data points and last longer than 66 μs, which are used to filter out noisy data. Finally, each data point cannot be separated by more than 1 ms. A pulse that meets these requirements is then saved with a start and end time.

Finally, to validate the technique, each pulse is matched to a detection from the two other independent lightning networks by time matching the cross-correlation pulses. A successful match is one where the network time occurs within the start and end time of pulse, accounting for the travel time to the sensor (0.3 ms) as well as the timing accuracy of the data, ranging from 1 ms to 1 second depending on the network.

IV. RESULTS AND DISCUSSION

Here we apply the detection technique to a single eruptive event from Bogoslof volcano in Alaska. Bogoslof is a volcanic island partially submerged beneath Bering Sea in the Aleutian Arc. Its eruption from December 2016 through August 2017 produced more than 60 volcanic ash plumes, many of which were electrified [Coombs et al., 2018]. One particularly well-characterized event occurred on June 10th, 2017 [Haney et al., 2018]. The seismic onset of this explosive eruption was 12:13:55 UTC and the event lasted until 14:51:18 UTC according to the U.S. Geological Survey's seismic network. During the event, LLS1 detected 31 strokes while LLS2 detected 6. The first discharge was detected by LLS1 and occurred at 12:16:16, approximately 2.5 minutes after the onset of seismic activity.

Results of the detections and cross-correlation are summarized in Table 1. Overall, we identified 552 pulses during the explosive event. Limiting to only the 10 minutes where LLS1 detected any activity, that overall count drops to 490. The peak in activity for LLS1 and pulses both agree at 12:50 UTC. Overall, this technique matches 88% of LLS1 and 100% of LLS2 detections. Furthermore, we detect significantly more discharges than the two independent networks, although many of these are likely to be false detections. This may be due to local noise sources as well as distant lightning that happens to also correlate with the same time difference.

TABLE I. CROSS-CORRELATION OF VOLCANIC LIGHTNING FROM THE JUNE 10TH 2017 ERUPTION OF BOGOSLOF VOLCANO IN ALASKA

Time (UTC)	LLS1 Stroke	LLS1 Match	LLS2 Stroke	LLS2 Match	Pulses (this method)
12:00	0	0	0	0	19
12:10	7	6	0	0	47
12:20	4	3	0	0	54
12:30	2	2	0	0	69
12:40	3	3	1	1	68
12:50	8	6	2	2	119
13:00	6	5	2	2	93
13:10	1	1	1	1	40
13:20	0	0	0	0	25
13:30	0	0	0	0	18
Total	31	26	6	6	552

Figure 2 illustrates an overview of all the data between 12:10 UTC and 12:20 UTC. The onset of the seismic activity occurred at 12:13:55 UTC (depicted by the vertical green line). The upper panel shows the waveform data from both sensors (UNLSK and USGS01).

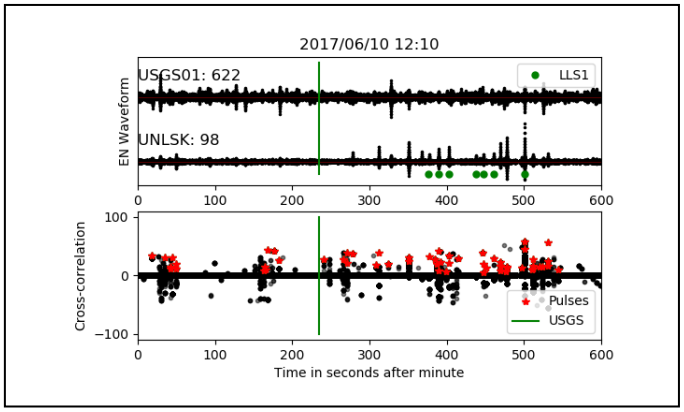

Figure 2. ENTLN waveform data from two ENTLN sensors (top) and their cross-correlation (bottom). The vertical green line represents the seismic onset time. The green dots represent the LLS1 reported times. The red stars represent the detected pulses from the cross-correlation technique. The y-axis is omitted on the upper panel because it was arbitrarily scaled to highlight the details. The lower panel shows the cross-correlations. The red stars are the cross-correlation pulses.

We can take a closer look at the first LLS1 detection, which is shown in Figure 3. Here, the green star is the beginning of the pulse and the red is the end. Considering the travel time and timing uncertainty from the LLS1 data, this is a positive match. The time difference between the two sensors is 1.7 ms, which is precisely the difference between the first waveform and the second and the reason for its designation as a pulse.

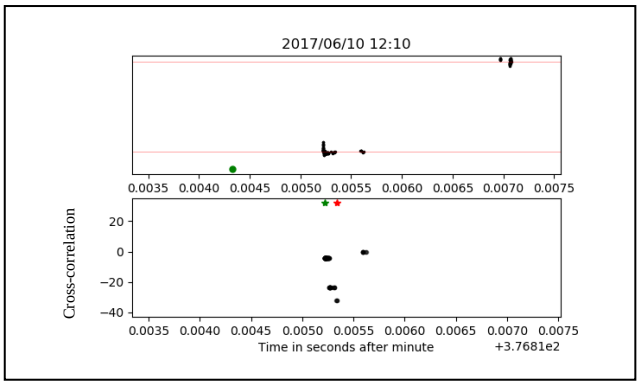

Figure 3. Similar format as Figure 2 with an example of first detection by LLS1 and matched cross-correlation pulse.

As mentioned, this technique is prone to false alarms. Figure 4 gives an example of this. These signals do not exhibit typical lightning discharge characteristices such as a clear, short duration peak (as in the top panel of Figure 3). Furthermore, the signal arrives at the more distant sensor before the closer sensor, meaning it is not coming from Bogoslof volcano. In the future, some of these key features could be used to identify and remove false alarms.

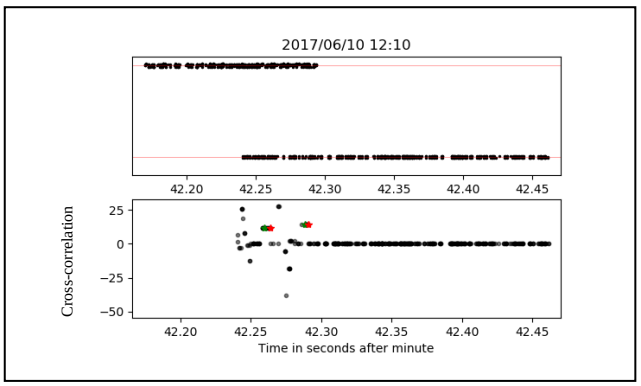

Figure 4. Example of first detection by LLS1 and matched cross-correlation pulse.

Figure 5 below shows an example of a LLS1 detection that was detected in the EN waveform data, but missed by the pulse categorization algorithm. These two signals are clearly correlated with a ~1.7 ms time difference, however the correlation is lower than one standard deviation, which was 4.5 ms in this case. Decreasing the threshold so that this pulse would have been accepted increases the number of pulses overall. It remains unclear whether these pulses are real or not.

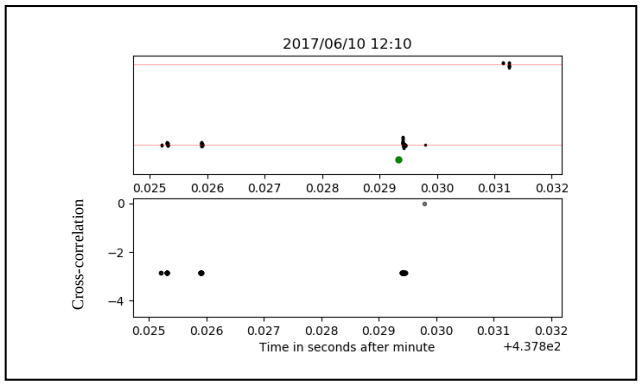

Figure 5. Example of a LLS1 detection that was missed.

Figure 6 shows three examples of cross-correlation pulses that are detected before the first LLS1 detection, but after the onset of seismic activity, and are discharges likely originating near Bogoslof volcano based on the time difference of the signals. The top example is the first pulse after the onset of seismic and occurred at 12:14:38 UTC, about 43 seconds after the onset of seismic activity. There are other pulses occurring sooner than this, however, based on their waveform characteristics those are thought to be false alarms due to noise.

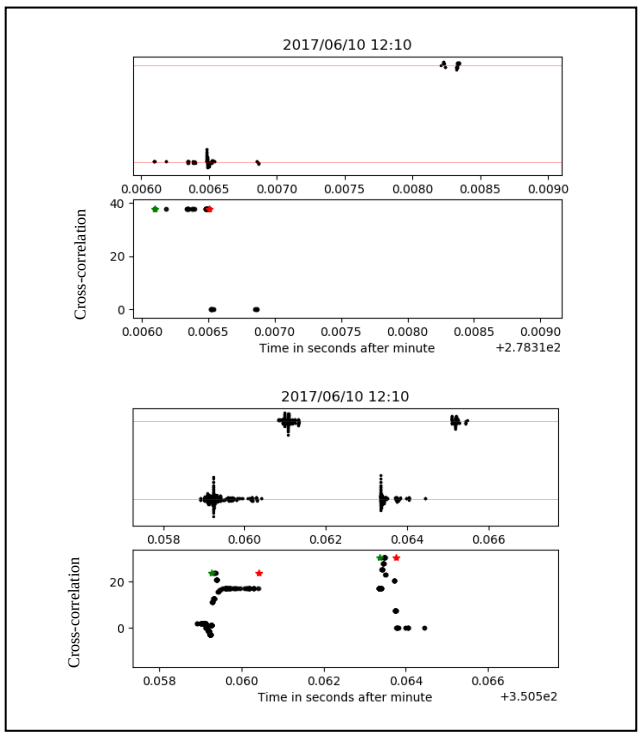

Figure 6. Three examples of cross-correlation pulses occurring before the first LLS1 detection that are possibly real lightning occurring near Bogoslof volcano.

Finally, we present an example of a possible lightning discharge that occurred before the seismic onset (Figure 7). This pulse likely occurred near Bogoslof based on the time difference between the two signals matching the expected travel time from the volcano. Despite being somewhat small in amplitude, this signal shows characteristics of a typical lightning discharge, short duration and distinctly peaked. It occurred at 12:10:18 UTC, about 3.5 minutes before the onset of seismic activity.

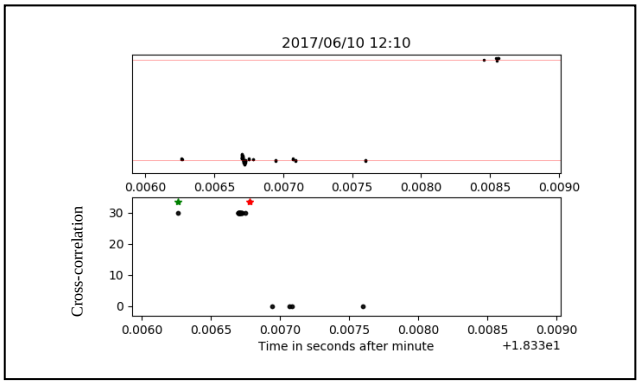

Figure 7. Possible volcanic discharge that occurred before seismic activity.

V. CONCLUSIONS

The goal of this study was to develop a new lightning detection technique that leverages the archived waveform data from electric field sensors operated by Earth Networks. This technique uses waveform data, a known location of interest, and cross-correlation technique to detect lightning occurring in the region of interest, in this case the Bogoslof volcano in Alaska. This technique is especially useful in remote regions where lightning detection networks are sparse, since only two sensors are required.

Results indicate that this technique detects >80% of the lightning located by independent networks. Furthermore, we identify significantly more pulses that were not detected by the other networks, many of which show indications of being real signals associated with the volcanic eruption. Some of these pulses occurred before the first detections of existing lightning networks, and some even before the onset of seismic activity, suggesting it could be a useful tool for early detection of explosive volcanism. Comparing the pulses with known detections reveals a number of characteristics that could be used to filter out false detections. For example, pulse length as well as cross-correlation wave shape could be used in the future to better exclude false alarms. Also, it was found that the current threshold can be lowered to include more LLS matches, however this may also increase the false alarm rate.

Initial results indicate that it is possible to obtain useful volcanic lightning data using only two sensors. This will be especially useful for detecting electrical activity from remote volcanoes that are not currently instrumented. Further work is needed to: (1) train the algorithm with other eruptive events to ultimately reduce the number of false detections, and (2) compare with other monitoring datasets to understand the physical source of the electrical pulses.

VI. ACHKNOWLEDGMENTS

Any use of trade, firm, or product names is for descriptive purposes only and does not imply endorsement by the U.S. Government.

REFERENCES

Behnke, S.A. and McNutt, S.R., 2014. Using lightning observations as a volcanic eruption monitoring tool. Bull. Volcanol., 76 (8), doi:10.1007/s00445-014-0847-1.

Behnke, S.A., Thomas, R.J., McNutt, S.R., Schneider, D.J., Krehbiel, P.R., Rison, W. and Edens, H.E., 2013. Observations of volcanic lightning during the 2009 eruption of Redoubt Volcano. J. Volcanol. Geotherm. Res., 259, 214-234, doi:10.1016/j.jvolgeores.2011.12.010.

Coombs, M.L., Wech, A.G., Haney, M.M., Lyons, J.J., Schneider, D.J., Schwaiger, H.F., Wallace, K.L., Fee, D., Freymueller, J.T., Schaefer, J.R. and Tepp, G., 2018. Short-Term Forecasting and Detection of Explosions During the 2016–2017 Eruption of Bogoslof Volcano, Alaska. Frontiers in Earth Science, 6, doi:10.3389/feart.2018.00122.

Drake, S.R. and Dogancay, K., 2004, May. Geolocation by time difference of arrival using hyperbolic asymptotes. In Acoustics, Speech, and Signal Processing, 2004. Proceedings.(ICASSP'04). IEEE International Conference on (Vol. 2, pp. ii-361). IEEE.

Fee, D., Haney, M.M., Matoza, R.S., Van Eaton, A.R., Cervelli, P., Schneider, D.J. and Iezzi, A.M., 2017. Volcanic tremor and plume height hysteresis from Pavlof Volcano, Alaska. Science, 355, 45-48.

Haney, M.M., Van Eaton, A.R., Lyons, J.J., Kramer, R.L., Fee, D. and Iezzi, A.M., 2018. Volcanic Thunder From Explosive Eruptions at Bogoslof Volcano, Alaska. Geophys. Res. Lett., 45 (8), 3429-3435, doi:10.1002/2017gl076911.

Liu, C., Sloop, C. and Heckman, S., Application of Lightning in Predicting High Impact Weather. TECO, 2014.

Thomas, R.J., McNutt, S.R., Krehbiel, P.R., Rison, W., Aulich, G., Edens, H.E., Tytgat, G. and Clark, E., 2010. Lightning and electrical activity during the 2006 eruption of Augustine Volcano. U.S. Geol. Surv. Prof. Paper, 1769, 579-608.

Zhu, Y., V. A. Rakov, M. D. Tran, M. G. Stock, S. Heckman, C. Liu, C. D. Sloop et al. "Evaluation of ENTLN Performance Characteristics Based on the Ground Truth Natural and Rocket‐Triggered Lightning Data Acquired in Florida." Journal of Geophysical Research: Atmospheres 122, no. 18 2017, pp. 9858-9866.